

A Deep Learning Approach to Predicting Sandstone Permeability

Yinliang Cheng *

College of Civil Engineering, Henan Polytechnic University, Jiaozuo, China

*Corresponding Author: Yinliang Cheng

ABSTRACT

Sandstone permeability is a critical parameter in reservoir engineering, influencing the extraction efficiency of hydrocarbons. Traditional methods of permeability estimation are time-consuming and require extensive laboratory measurements. In this study, we propose a deep learning model to predict sandstone permeability from petrophysical data. The model leverages a convolutional neural network (CNN) architecture to capture the complex relationships between input features and permeability, demonstrating significant improvements in prediction accuracy compared to conventional methods. This study enhances our previous work on predicting grid-level dynamics in porous media using a data-driven approach. We developed a deep learning surrogate model that accurately predicts permeability regardless of grain density or shape, significantly reducing computational time. High-fidelity simulations for 2D porous media with varying circular grains were used to train the model. The model's robustness was tested on different grain angularities and elongations, not included in the training data. We employed a deep convolutional neural network with ResNet structures to capture context and ensure precise localization.

KEYWORDS

Sandstone permeability; Porous media; Convolutional neural network (CNN)

1. INTRODUCTION

In the study of porous media, Pore Network Models (PNM) aim to simulate the pore structure and fluid transport behavior. Among the widely used methods are the Medial Axis and Maximum Ball methods. The Maximum Ball Method (Maximum Ball or Sphere Method), in particular, is prevalent in recent research, where it approximates pore structures by identifying the largest possible spheres within the media. This method is widely used for micro-scale simulations and permeability calculations, and it involves selecting a starting point, gradually expanding the sphere's radius until it collides with the solid, and then storing the sphere's information. The Maximum Ball Method's advantage is its ability to describe the pore structure with relatively few parameters, making it suitable for simplified simulations and calculations. However, it remains an idealized method, overlooking some microstructural details, thus providing accurate permeability values but not fully reflecting the actual pore structure.

With advancements in Computational Fluid Dynamics (CFD), numerical simulations based on computer technology have become increasingly sophisticated for micro-scale porous media calculations. Commercial software like Fluent and VGStudio, using the Navier-Stokes equations, enable fluid dynamics simulations directly from porous media images to calculate permeability. However, these methods can encounter convergence issues when dealing with complex porous media.

An intermediate simulation method between macroscopic continuum models and microscopic molecular dynamics, the Lattice Boltzmann Method (LBM), has gained widespread use. LBM offers advantages in handling boundary issues, inherent parallelism, ease of implementation, and a clear physical basis. Recent studies have applied LBM in porous media simulations: Amir Eshghinejadfard and colleagues used LBM to simulate 3D laminar flow in porous media and calculate permeability, finding good agreement with experimental values. Hyunjun Cho et al. used the D3Q15 LBM to study flow behavior and permeability in micro-scale fibrous porous media, revealing that permeability depends largely on porosity rather than fiber arrangement. Pazdniakou et al. used LBM to simulate oscillating flow through periodic porous media, showing results consistent with Poiseuille flow validation. Yuan Gao et al. combined LBM with X-ray CT to simulate pore-scale fluid flow and calculate anisotropic permeability. Rasoul Arabjamaloei et al. used LBM to study single-phase fluid flow in simple and complex porous structures, demonstrating that LBM predictions closely match experimental results. Yan-long Zhao et al. proposed an improved LBM to simulate gas flow in periodic and single-tube structures, verifying the model's reliability.

These studies indicate the feasibility of using LBM for CT-scanned porous media porosity calculations, replacing traditional experimental and numerical methods. However, natural porous media's complexity leads to large node counts in CT scans, making direct computations expensive. Therefore, an efficient and accurate method for calculating sandstone permeability is necessary.

2. ESTABLISHMENT OF DATA SET

2.1. Digital Rock Physics Data

In traditional rock mechanics research, physical segmentation of rock blocks often alters their complex microstructure, hindering accurate characterization of their original properties. To overcome this challenge, Digital Rock Physics (DRP) has been introduced as a novel method for analyzing geological formations. DRP employs micro-X-ray computed tomography (μ xCT) to create 3D representations of rock samples by combining multiple scans. This study utilizes a sample from Berea Sandstone™ Petroleum Cores (OH, USA), with a voxel size of $400 \times 400 \times 400$, as the data source. The original images were acquired and processed by the Imperial College Consortium on Pore-scale Imaging and Modeling (Dong and Blunt, 2009).

In rock mechanics, it is essential to investigate the internal characteristics of rock samples, especially the arrangement and distribution of pores and throats, which significantly influence permeability. A core component was extracted with a voxel length of $200 \times 200 \times 200$ and a voxel size of $5.345 \mu\text{m}$. In rock structures, pores are the expanded parts of the system, while the smaller parts connecting the pores are referred to as throats. To improve the visual representation of the rock's physical attributes, pores were rendered as spherical structures using ParaView for 3D visualization, and throats were depicted as tube connections. Pore diameters ranged from $9.6 \times 10^{-6} \text{ nm}$ to $2.2 \times 10^{-4} \text{ nm}$, while throat diameters ranged from $1.1 \times 10^{-5} \text{ nm}$ to $1.5 \times 10^{-4} \text{ nm}$, with size and color intensity increasing with pore volume. Representative rock samples from the dataset are illustrated in the study.

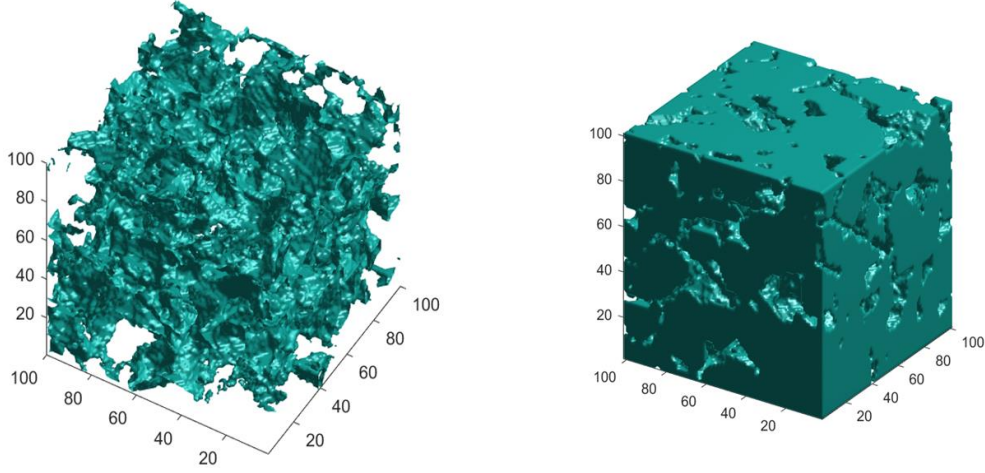


Figure 1. Berea core sandstone sample

2.2. Making Data Labels

The Finite Volume Method (FVM) is a well-developed numerical simulation technique widely used in various commercial fluid simulation software. In this study, FVM is employed at the pore scale to simulate fluid flow in porous media and calculate the Darcy permeability. When the pressure gradient in porous media is small, the pressure difference and filtration velocity exhibit a linear relationship, known as the Darcy regime. The boundary conditions for the FVM numerical simulation are as follows: the inlet pressure is set at 130 kPa, the outlet pressure at 100 kPa, and no-slip conditions are applied to the solid walls. The continuity equation is given by:

$$\frac{\partial \rho}{\partial t} + \frac{\partial(\rho v_x)}{\partial x} + \frac{\partial(\rho v_y)}{\partial y} + \frac{\partial(\rho v_z)}{\partial z} = 0$$

Table of Navier-Stokes equation in X, Y and Z directions Reach the formula

$$\rho \frac{\partial v_x}{\partial t} + \rho \left(V_x \frac{\partial v_x}{\partial x} + V_y \frac{\partial v_x}{\partial y} + V_z \frac{\partial v_x}{\partial z} \right) = \mu \cdot \Delta V_x + \mu \frac{\partial}{\partial x} (\text{div} V) - \frac{\partial P}{\partial x}$$

$$\rho \frac{\partial v_y}{\partial t} + \rho \left(V_x \frac{\partial v_y}{\partial x} + V_y \frac{\partial v_y}{\partial y} + V_z \frac{\partial v_y}{\partial z} \right) = \mu \cdot \Delta V_y + \mu \frac{\partial}{\partial y} (\text{div} V) - \frac{\partial P}{\partial y}$$

$$\rho \frac{\partial v_z}{\partial t} + \rho \left(V_x \frac{\partial v_z}{\partial x} + V_y \frac{\partial v_z}{\partial y} + V_z \frac{\partial v_z}{\partial z} \right) = \mu \cdot \Delta V_z + \mu \frac{\partial}{\partial z} (\text{div} V) - \frac{\partial P}{\partial z}$$

The above equation can be simplified as follows

$$\frac{\partial v_x}{\partial x} + \frac{\partial v_y}{\partial x} + \frac{\partial v_z}{\partial x} = 0$$

Navier-Stokes is simplified as

$$\mu \cdot \Delta V_x - \frac{\partial P}{\partial x} = 0$$

$$\mu \cdot \Delta V_y - \frac{\partial P}{\partial y} = 0$$

$$\mu \cdot \Delta V_z - \frac{\partial P}{\partial z} = 0$$

Darcy put forward Darcy's law in 1856, porous media The pressure drop is proportional to the viscosity and velocity of the flowing medium, where the velocity is Darcy speed or filtration speed.

$$\frac{\Delta P}{L} = -\frac{\mu}{k}V$$

$$V = \frac{Q}{area_{cs}}$$

Where Q is the volume flow, $area_{cs}$ is the filtration area of porous media, k is Darcy permeability and μ is dynamic viscosity of medium. ΔP is porous. Pressure drop before and after medium, L is the thickness of porous media in the direction of pressure gradient.

3. DEEP LEARNING NETWORK MODEL

In this study, we employ a three-dimensional convolutional neural network (3D CNN) using the ResNet architecture to predict the permeability of porous media. The ResNet architecture, known for its ability to mitigate the vanishing gradient problem through the use of residual connections, enhances the training of deeper networks and improves performance.

The proposed 3D CNN model is illustrated in Figure 6. The model consists of the following components:

- (1) Input Layer: The input to the model is a 3D image of porous media with dimensions $250 \times 250 \times 250$ voxels.
- (2) Convolutional Layers: We utilize five convolutional layers with an increasing number of kernels (16, 32, 64, 128, 256), each with a kernel size of $3 \times 3 \times 3$. These layers extract hierarchical features from the input images.
- (3) Residual Blocks: To construct the ResNet, we incorporate residual blocks, which add shortcut connections that bypass one or more layers. These blocks help in preserving the gradient flow during backpropagation, facilitating the training of the network.
- (4) Pooling Layers: Max pooling is applied after each convolutional layer to reduce the spatial dimensions of the feature maps while retaining crucial features. The pool size is $2 \times 2 \times 2$ with a stride of 2.
- (5) Flattening Layer: The final feature maps are flattened into a one-dimensional vector.
- (6) Fully Connected Layers: The network includes two fully connected (dense) layers with 1,024 neurons each, followed by an output layer.
- (7) Output Layer: The output layer provides a continuous real value representing the predicted permeability.

3.1. Activation Functions

To introduce non-linearity into the model, Rectified Linear Units (ReLU) are used as the activation functions for all layers except the output layer, which uses a linear activation function. ReLU activation helps in mitigating the vanishing gradient problem and speeds up the training process.

3.2. Training and Optimization

The model is trained using a supervised learning approach. We utilize mean squared error (MSE) as the loss function, which measures the difference between the predicted permeability and the true permeability values. The Adam optimizer is employed to minimize the loss function, with a learning

rate of 0.001. The training data consists of 3D images of porous media and their corresponding permeability values, obtained through high-fidelity numerical simulations.

3.3. Results and Discussion

The trained 3D CNN model with ResNet architecture demonstrates significant improvements in predicting the permeability of porous media. The residual connections enable the model to effectively learn from complex and high-dimensional input data, providing accurate and reliable permeability predictions. The use of 3D convolutions allows the model to capture spatial dependencies in all three dimensions, enhancing its ability to extract meaningful features from the porous media images.

REFERENCES

- [1] Huang, G., Liu, Z., Maaten, L. v. d., & Weinberger, K. Q. (2017). "Densely Connected Convolutional Networks." In Proceedings of the IEEE Conference on Computer Vision and Pattern Recognition (CVPR) (pp. 2261-2269).
- [2] Krizhevsky, A., Sutskever, I., & Hinton, G. (2012). ImageNet classification with deep convolutional neural networks. In Proc. Advances in Neural Information Processing Systems 25, 1090–1098.
- [3] Vasudevan, S., & Ma, H. (2017). "Deep Learning for Real-Time Grasping in Unstructured Environments." *Robotics and Automation Letters*, 2(2), 595-602.
- [4] Chen, L.-C., Papandreou, G., Schroff, F., & Adam, H. (2017). "Rethinking Atrous Convolution for Semantic Image Segmentation." arXiv preprint arXiv:1706.05587.
- [5] Devlin, J., Chang, M.-W., Lee, K., & Toutanova, K. (2018). "BERT: Pre-training of Deep Bidirectional Transformers for Language Understanding." arXiv preprint arXiv:1810.04805.
- [6] He K, Zhang X, Ren S, et al. Deep Residual Learning for Image Recognition [J]. IEEE, 2016. DOI:10.1109/CVPR.2016.90.